Experimental Thermal and Fluid Science 108 (2019) 61–74

Contents lists available at ScienceDirect

Experimental Thermal and Fluid Science

journal homepage: www.elsevier.com/locate/etfs

Micro-grooved surfaces to enhance flow boiling in a macro-channel

Maria C. Vlachou[a], Chara Efstathiou[b], Aristomenis Antoniadis[b], Thodoris D. Karapantsios[a,*]

[a] Faculty of Chemistry, Division of Chemical Technology, Aristotle University of Thessaloniki, University Box 116, 54124 Thessaloniki, Greece
[b] School of Production Engineering & Management, Technical University of Crete, Chania, Greece

ARTICLE INFO

Keywords:
Passive enhancement technique
Laser etching
Surface treatment
Flow boiling incipience
Heat transfer coefficient
Bubble dynamic behavior

ABSTRACT

The influence of the boiling surface morphology on subcooled flow boiling heat transfer is investigated. Flow boiling experiments are conducted in a macro-channel with water entering at 30 °C. The channel has an orthogonal cross-section (10x40 mm) with a short (length: 120 mm) one-sided heated wall. Experiments are performed at two flow directions, horizontal and vertical upward. The examined mass and heat fluxes range between 330–830 kg/m^{2}s and 200–1000 kW/m^2, respectively. Two copper boiling surfaces are manufactured by laser etching: one with micro-grooves parallel to the flow direction (surface #1) and one with micro-grooves perpendicular to the flow direction (surface #2). The grooves have the same width (420 μm) and depth (290 μm) but their length varies: 100 mm along the channel's length (surface #1) and 30 mm across the channel's width (surface #2). The presence of grooves yields ~ 8% increase of heat exchange area in both surfaces. A smooth plain copper surface is employed as reference. Micro-grooves lead to boiling inception at lower wall superheats (−70% for horizontal and −30% for vertical channel inclination) and also enhance heat transfer coefficients (10–15% for horizontal and 5–7% for vertical channel inclination) compared to the smooth surface; this is for two reasons: (a) laser etching creates micro-scale-roughness inside the grooves, which provide more active bubble nucleation sites, and (b) the bottom of the grooves is hotter than the rest of the surface. As a result, many bubbles are generated inside the grooves, where they grow and coalescence with other bubbles at a greater extent than the rest of the boiling surface. The beneficial effect of the grooved surfaces is beyond the gain offered by the rise in surface area and it is seen mainly in the horizontal inclination, whereas it is less evident in the vertical inclination. This is comparable with the discrepancy observed between inclinations for the smooth boiling surface.

1. Introduction

Boiling is one of the most popular means of heat transfer and is encountered in applications such as steam production, cooling of high power electronics and thermal management in general. Although its mechanism is complex, it appears to be a very efficient process. The reason is that it combines evaporation, conduction, convection and turbulent mixing within a hot liquid layer close to the boiling surface (thermal boundary layer) [1]. Several techniques (passive or active) have been proposed in literature to alter the "micro-environment" within the boundaries of the thermal boundary layer and so enhance heat transfer [2]. The simplest and easiest way of boiling (pool and flow) enhancement according to many authors [3–5] is by modifying the boiling surface's geometry/structure. Each surface modification enhancement method as applied to a specific system of fluid/boiling surface, may have different effects on the heat transfer mechanism, e.g., (a) increase of the heat exchange area and/or density of active nucleation sites, (b) increase of surface roughness/porosity and, consequently, promotion of turbulence and/or change of the velocity profile inside the thermal boundary layer.

So far several researchers have shown a clearly improved performance when they applied micro-structured surfaces to boiling, constructed by various methods. For instance, in flow boiling, Ω-shaped grooves were found to increase heat transfer coefficient by about 1.5–3.3 times [6]; honeycomb structured surfaces produced by sintering were found to enhance CHF 1.1–2.4 times [7]; micro-channel structures milled on tubes showed a 5.2–18.1% increase in CHF [8]. On the other hand, in pool boiling, micro-grooves of various widths and heights manufactured by CNC were seen to increase CHF up to 160% [9].

Among the different surface modification techniques to produce micro-grooved surfaces for boiling, there has been emerging interest in simple engraving methods, such as lithography or laser etching; yet only a few published works can be found in literature. Regarding flow

* Corresponding author.
E-mail address: karapant@chem.auth.gr (T.D. Karapantsios).

https://doi.org/10.1016/j.expthermflusci.2019.05.015
Received 10 October 2018; Received in revised form 19 May 2019; Accepted 21 May 2019
Available online 22 May 2019
0894-1777/

Nomenclature

A	heat exchange area, m^2
CA	contact angle, ^{o}
C_p	specific heat, $J\,kg^{-1}\,K^{-1}$
D_h	hydraulic diameter, m
f	Darcy friction factor, –
G	mass flux, $kg\,m^{-2}\,s^{-1}$
h	heat transfer coefficient, $W\,m^{-2}\,K^{-1}$
k	thermal conductivity, $W\,m^{-1}\,K^{-1}$
L	channel length, m
P	pressure, bar
Q	heat flow, W
Pr	Prandl number ($C_p\,\mu\,k^{-1}$), –
q"	heat flux, $W\,m^{-2}$
Re	Reynolds number ($\rho\,u\,D_h\,\mu^{-1}$), –
T	temperature, ^oC
u	velocity, $m\,s^{-1}$
w	channel width, m
x	channel height, m

Greek symbols

ΔT	temperature difference, ^oC
Δh	heat transfer coefficient difference, $W\,m^{-2}\,K^{-1}$
η	enhancement factor, %
μ	dynamic viscosity, $N\,s\,m^{-2}$
ρ	density, $kg\,m^{-3}$

Subscripts

ave	average
CHF	critical heat flux, $W\,m^{-2}$
exp	experimental
f	film
FC	forced convection
in	inlet
l	liquid
mix	mixing cup
modified	modified surface (gooved)
OBR	Onset of Bubbly Regime
ONB	Onset of Nucleate Boiling
out	outlet
sat	saturation
s	smooth surface (reference)
sub	subcooling
theor	theoretical
wall	heated wall

boiling, Sommers and Yerkes [10] used two different techniques, standard photolithography and laser etching, to create grooves on an aluminum boiling surface (24 cm^2). The grooves had a width of 17.7 and 50 μm and a depth of 12.2 and 10 μm, respectively, for the two methods, and were perpendicular to the flow. These authors examined flow boiling inside a macro-channel (x: 3 mm, w: 31.75 mm, L: 63.5 mm) using R-134a as working fluid with mass fluxes between 100 and 600 kg/m^2s. The laser etched surface showed a 90–100% enhancement of heat transfer coefficient, while the surface modified by photolithography showed an enhancement of only 35–48%. The different performance of the two surfaces was attributed to the unique micro-structural characteristics of the laser etched surface; a porous microstructure was created in the grooves with nano-scale roughness which provided numerous active nucleation sites and also helped keeping these sites wetted by capillarity. Yet, the authors based their analysis on SEM, which allows arguments about nano-scale roughness but it not suitable to judge about porosity. Anyway, the above indicate that fabrication of the boiling surface is important in the overall flow boiling heat transfer performance and that laser etching can be considered as an extremely efficient enhancement method for metallic surfaces. However, grooves with width and depth of just a few tenths of micros can be etched only in hard metals such as aluminum and stainless steel.

Regarding pool boiling, Rahman et al. [11,12] constructed grooves (width: 420 μm, depth: 290 μm) on copper surfaces by wire electrical discharge machining with a varying inter-groove distance between 0.78 and 3.28 mm and conducted saturated pool boiling experiments with water. They used surfaces either bare or covered with a porous coating or with the grooves filled with a non-conductive epoxy layer. The presence of these micro-grooves has led to a remarkable 2.6 times enhancement in CHF and heat transfer coefficient across the entire boiling curve in all examined cases. This was attributed to increased nucleation rate at lower superheats and enhanced bubble dynamics inside the grooves.

In the current work, laser etched grooves on copper boiling surfaces are examined at demanding flow boiling conditions in order to asses for the first time the possibility of noteworthy heat transfer enhancement by simple surface modification techniques. The examined working conditions refer to the simultaneous existence of high heat fluxes (200–1000 kW/m^2), high mass fluxes (330–830 kg/m^2s) and high inlet subcooling (70°C). Such conditions are encountered in emergency efforts to remove high heat loads, e.g. of a sudden fire, from closed spaces by rushing large amounts of ambient water along the external side of their walls. Such an emergency has been a hypothetical scenario for a fire in a room of the International Space Station where used/dirty water from storage tanks could be hurriedly flow through the hollow metallic walls to cool them down until astronauts leave the room. Experiments are performed with water at two flow directions, horizontal and vertical upwards. The scope of this work is to examine the effect of grooves on flow boiling incipience, boiling curves, and two-phase heat transfer coefficient in the region where nucleate boiling mechanism dominates (away from the region of critical heat flux). This is a part of a series of works examining various parameters (i.e. mass flux, heat flux, channel size, channel inclination, gravity) at these demanding working conditions. Heat transfer results are combined with visual observations of bubbles interaction to provide an insight about the heat transfer mechanism.

2. Experimental methodology

2.1. Flow boiling loop

Experiments are performed at a flow boiling loop (Fig. 1a), which allows simultaneous flow rate, temperature and high speed video recordings; a detailed description is provided in Vlachou, et al. [13]. Deionized water circulated by a progressive cavity pump (Sydex, K-032-1S, 1 hp) is the working fluid. The test section consists of a channel of orthogonal cross-section (height 10 mm, width 40 mm) with a heated length of 120 mm and a non-heated entrance length of 500 mm. The test section is based on a precision rotation unit that allows changing channel's inclination around a full circle; at the present study only horizontal (0°) and vertical upward (90°) flows are examined. The channel consists of the boiling surface at the bottom of the channel (one-side heating; copper block with 14 cartridge heaters, max heat capacity 5.5 kW) and an aluminum frame with embedded glass windows covering the other three sides to allow optical observations of bubbles activity (Fig. 1b).

Volumetric flow rate is measured by a paddle wheel transmitter

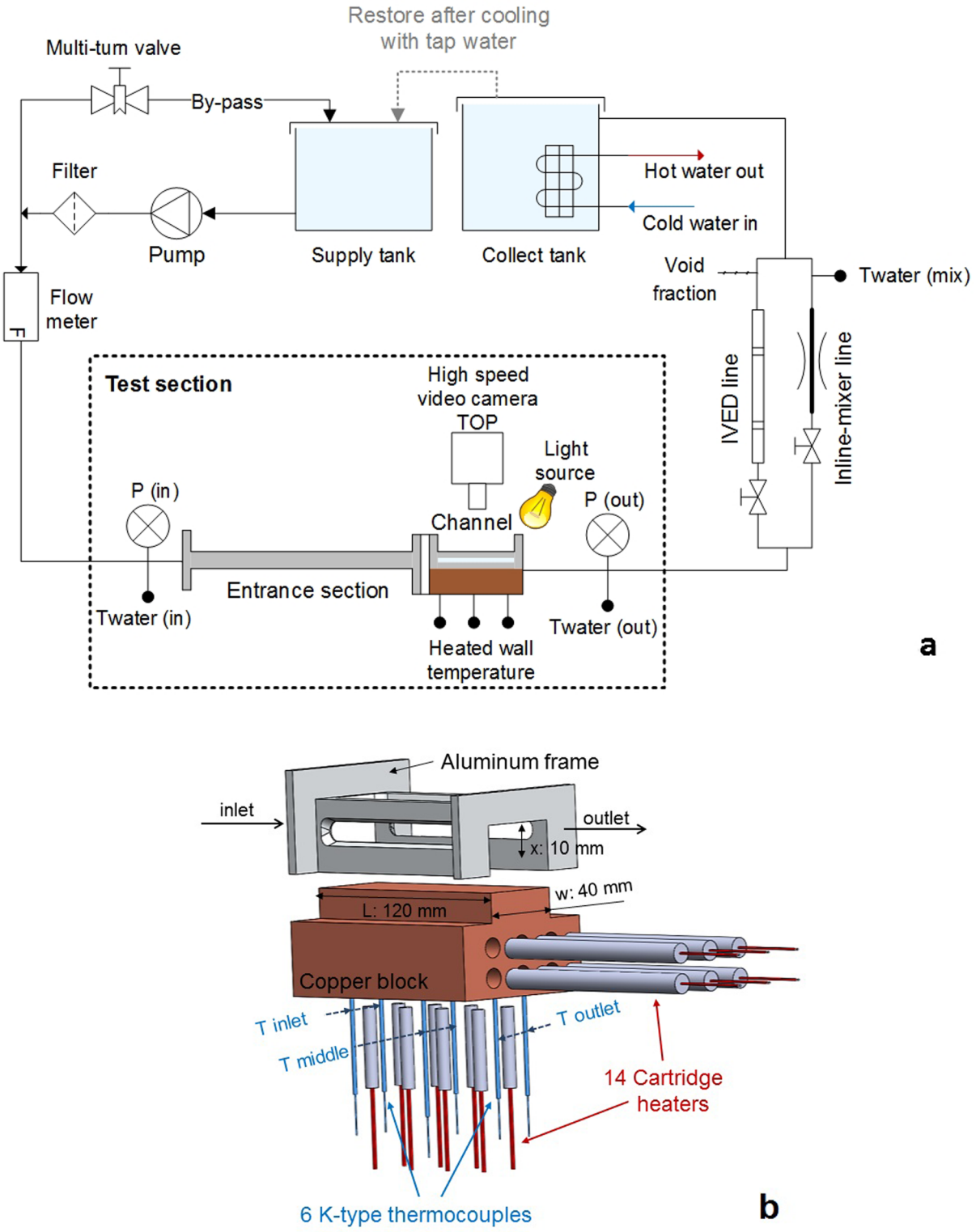

Fig. 1. Schematic diagram of (a) the flow boiling experimental setup and (b) the test section.

(Burkert 8035, range 0.3–10 m/s, accuracy ± 2.5% of measured value). Temperatures of the working fluid and the heated wall are obtained by K-type, ungrounded thermocouples (Uteco, 2 mm, accuracy after calibration ± 0.1 °C). Working fluid's inlet temperature (T_{in}) is acquired prior the entrance section whereas its outlet mixing cup temperature is acquired right after an inline static mixer (Koflo, 1 in − 6 elements) (T_{mix}). The installation of an in-line mixer at the channel's outlet is necessary in order to acquire a mass flow averaged water temperature. The temperature inside the copper block is measured at 6 positions; five of them 2 mm below the boiling surface and one 12 mm below the boiling surface. High speed imaging is realized through the top wall of the channel with a high speed video camera (Mikrotron, Motionblitz, Eosens mini 2, 60 mm macro lens, 8000–10,000 fps) 10 mm before the channel's exit. Experiments begin by starting the pump and adjusting the flow rate to the desired value. Next the heater is powered at a certain value. Heat flux is tuned by activating different

Table 1
Working conditions.

Parameter	Value/ Range	Unit
Subcooling inlet, $\Delta T_{sub,in}$	70	°C
Subcooling outlet, $\Delta T_{sub,out}$	62.9–69.7	°C
Mass fluxes, G	330, 630, 830	kg/m^2 s
Liquid velocity, u_l	0.33, 0.63, 0.83	m/s
Heat fluxes, q"	200–1000	kW/m^2
Channel dimensions	x10, w40, L120	mm
Inclinations	0, 90	°

combinations of cartridge heaters every time and by fine adjustment of the supplied voltage with a variac controller.

All experiments are conducted at nearly atmospheric pressure and proper recordings of flow rate, temperature and high speed videos are made at steady state conditions, which are realized by the less than 0.1 °C deviation of the monitored heated wall temperature. At least three runs at every set of experimental conditions are conducted to estimate precision (repeatability); error bars are included in all plots presenting data markers. Table 1 summarizes the employed working conditions.

2.2. Surface preparation

Two different boiling surfaces are manufactured. These are termed as surface #1 (microgrooves parallel to the flow) and surface #2 (microgrooves perpendicular to the flow). These micro-grooved surfaces are examined in the test section in conjunction to a reference, smooth, copper surface (Table 2). The grooves are 420 μm wide and 290 μm deep and the surface area ratio of the two grooved surfaces versus the reference surface is approximately the same, $A_{modifeid}/A_s = 1.08$. The shape of the grooves is shown in Fig. 2a, b and c; the geometry is similar to that of Rahman et al. [11,12]. The grooves are engraved onto two different copper blocks (Fig. 2d and e) by laser etching (Lasertec 40, Sauer GmbH).

Regarding the morphology of the grooves, it is seen in Fig. 2 that laser etching on the one hand has created a micro-scale rough structure inside the grooves and on the other hand has caused an unavoidable deformation along the rims of the grooves, where a “bump” of melted material has gathered. As a result, the micro-grooved surfaces present increased roughness at those points and plenty of imperfections that can act as active nucleation sites [14].

Another aspect of surface morphology is the fact that polished copper is subject to oxidation when exposed to water flow boiling. On one hand, aging changes the wettability of copper surface (oxidized copper is less hydrophilic), and on the other hand, aging decreases copper’s conductivity (the oxidized copper layer inhibits heat transport from the copper surface to the liquid) (Supplementary 1). Aging results in a 10% reduction of the heat flux that passes via conduction from the heaters to the working fluid, i.e. decreases macro-channel’s heat transfer capacity, but it is inevitable. The detrimental effect of aging on our boiling surfaces has been previously examined [13], so it is made sure here that the boiling surfaces under examination have reached a steady state in terms of aging which is achieved after 48 h of boiling operation.

Supplementary data associated with this article can be found, in the online version, at https://doi.org/10.1016/j.expthermflusci.2019.05.015.

2.3. Data reduction

Calculations for the measured temperatures include:

T_{ave} is the average bulk liquid temperature along the channel (between the entrance and the mixing cup measuring station)

$$T_{ave} = \frac{T_{in} + T_{mix}}{2} \tag{1}$$

T_{wall} is the average wall temperature of the heated surface calculated from measurements at five locations along the heated surface. Measurements are taken 2 mm below the heated surface from which the temperature of the heated surface is estimated using Fourier law.

T_f is the film temperature between bulk liquid and hot wall, ΔT_{sub} is the degree of subcooling at the channel entrance and ΔT_{wall} is the wall superheat.

$$T_f = \frac{T_{wall} + T_{ave}}{2} \tag{2}$$

$$\Delta T_{sub} = T_{sat} - T_{in} \tag{3}$$

$$\Delta T_{wall} = T_{wall} - T_{sat} \tag{4}$$

Heat flux, q″ (=Q/A), is calculated by Fourier law using the temperature difference between the two thermocouples positioned at mid distance along the heated surface at 2 and 12 mm below the heated surface.

The average flow boiling heat transfer coefficient, h, is calculated as:

$$h = \frac{q''}{T_{wall} - T_{ave}} \tag{5}$$

The enhancement percentage of heat transfer coefficient is obtained from:

$$\eta = \frac{h_{modified} - h_s}{h_s} \cdot 100 \tag{6}$$

The empirical model used for comparisons in single phase forced convective flow is (Gnielinski [15] (± 15%)):

$$h_{FC} = \frac{Nu \cdot k}{D_h}; \quad Nu = \frac{\frac{f}{8}(Re - 1000)\cdot Pr}{1 + 12.7\left(\frac{f}{8}\right)^{\frac{1}{2}}\left(Pr^{\frac{2}{3}} - 1\right)}; \quad D_h = \frac{2xw}{x+w} \tag{7}$$

Mean absolute percentage error (MAPE) between the entire experimental, h_{exp}, dataset and the respective predicted values, h_{theor}, is calculated from:

$$MAPE = \left[\frac{1}{N}\sum_{1}^{N} ABS\left(\frac{h_{theor} - h_{exp}}{h_{exp}}\right)\right] \cdot 100 \tag{8}$$

Table 2
Characteristics of the examined boiling surfaces.

Surface	Material	Geometry	Width (mm)	Depth (mm)	Length (mm)	Step (mm)	No of grooves	Surface area (mm^2)	Ratio A/A_s
Smooth	Cu	Untreated (reference)	–	–	–	–	–	4800	1.000
Surface #1	Cu	Grooves parallel to the flow	0.42	0.29	100	3.7	9	5200	1.083
Surface #2	Cu	Grooves perpendicular to the flow	0.42	0.29	30	3.7	28	5170	1.077

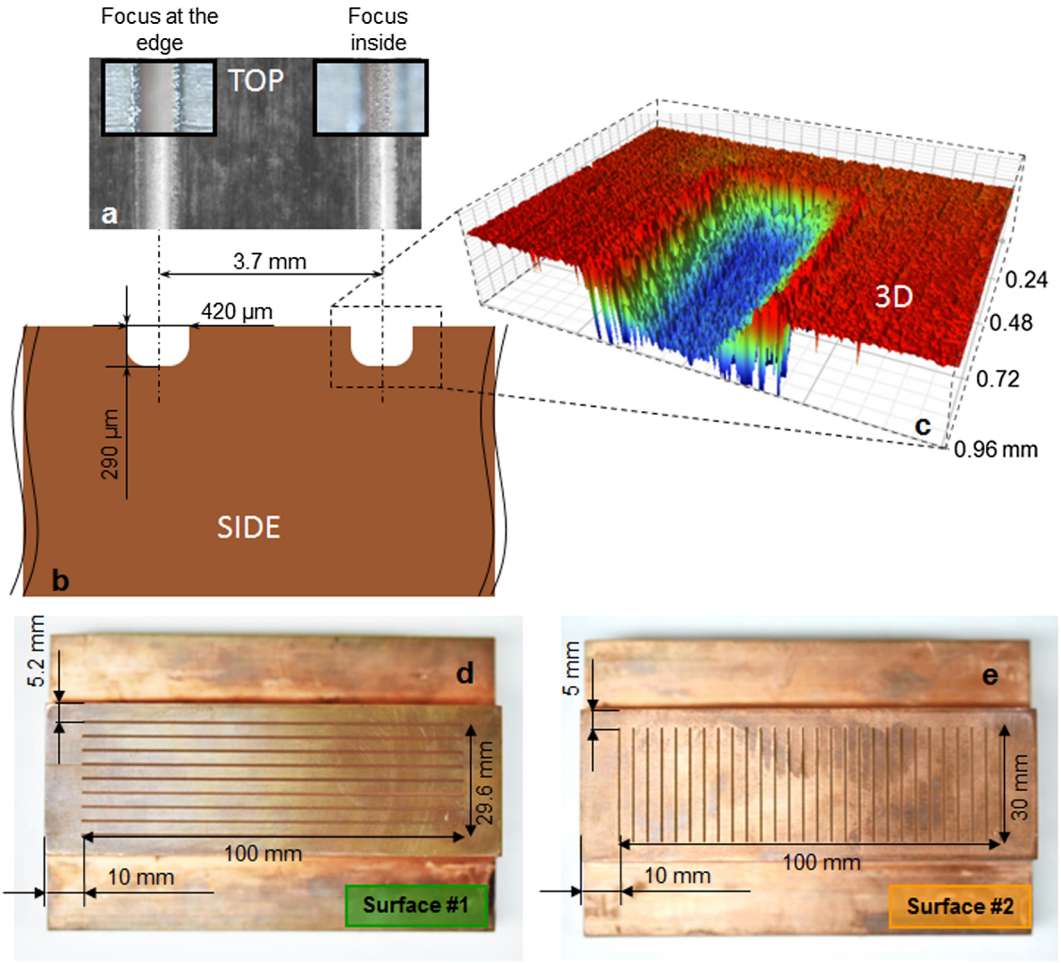

Fig. 2. Boiling surface with microgrooves: (a) top photo (b) side schematic diagram (c) 3D profilometer view of the grooves, (d) photograph of surface #1, and (e) photograph of surface #2.

Table 3
Measurement error and uncertainties.

Parameter	Range	Error (%)	Parameter	Uncertainty (%)
Temperature	25–150 °C	± 0.1	Heat flux, q"	± 0.15
Volumetric flow rate	8.1–19.7 L/min	± 2.5	Mass flux, G	± 3
Channel dimensions	3–120 mm	± 0.05	Heat transfer coefficient, h	± 2.5

2.4. Uncertainty analysis

All measuring sensors (flow rate, pressure, temperature) are calibrated before they are used in the experiments. The measurement errors and uncertainty propagated in the calculated parameters are provided in Table 3. Errors in the measured parameters are obtained from repeatability tests via root sum square method and the uncertainties associated with dependent parameters are calculated using standard error analysis [16].

2.5. Single phase and two phase validation

Single phase heat transfer experiments are performed at low q" conditions (below the Onset of Boiling, ONB) for the three surfaces (smooth, surface #1, surface #2), three mass fluxes (330, 630 and 830 kg/m^2 s) and two inclinations (horizontal and vertical). Heat losses are estimated at about 6.5% as the difference between the heat generated by the cartridge heaters and the heat received by the water flow [13]. The experimental heat transfer coefficient is compared with the one predicted by Gnielinski's empirical model in Fig. 3a for the smooth surface and Fig. 3b for the modified surface. As can be seen, experimental data lie between 0 and −40% but the majority of the data are close or better than the −15% tolerance of the model (top dashed line in the graphs of Fig. 3) with a MAPE of 15%. It must be added here that two phase heat transfer coefficients for the smooth surface have been previously examined and have shown fair agreement with the empirical models of Liu-Winterton [17] and Shah [18] (MAPE values for the two models were 31.9% and 21.1%, respectively, which were both within the tolerance of those models) [19].

3. Results and discussion

3.1. Effect of surface morphology on bubble dynamics

Bubbles' dynamic behavior on a smooth boiling surface has been studied previously [19]. On an aged (oxidized), copper, smooth boiling surface (reference for comparisons with the present modified surfaces) two types of bubbles behavior dominate.

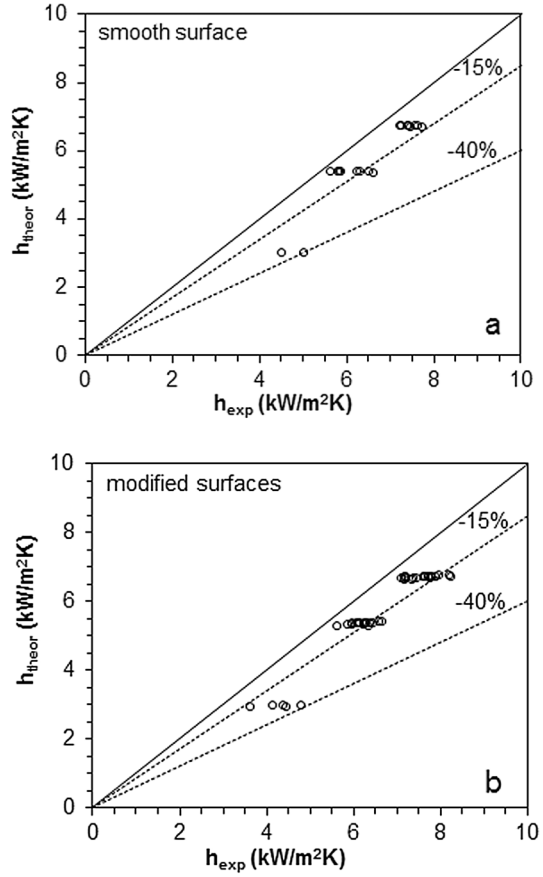

Fig. 3. Single phase validation of experimental heat transfer coefficient with Gnielinski's empirical model for (a) smooth and (b) modified surfaces.

The first type refers to bubbles of various sizes that slide at different speeds along the boiling surface with their size oscillating around an average size. Such bubbles constitute the vast majority on the boiling surface. When sliding bubbles meet each other, they coalescence, but the new large bubble does not grow much larger; instead, it condenses down to a size similar to the initial bubbles' sizes. Representative behavior of sliding bubbles on a smooth surface at horizontal channel inclination is shown in Supplementary 2. This has been argued as the basic heat transfer mechanism of subcooled flow boiling for the specific experimental conditions [19]. The second type of bubbles refers to stagnant bubbles (pinned at their nucleation site) that grow with time until they get large enough and suddenly detach and fully condense in the surrounding cold bulk liquid. Such bubbles are apparently anchored at tiny imperfections of the smooth surface and are much less in number than those of the first type.

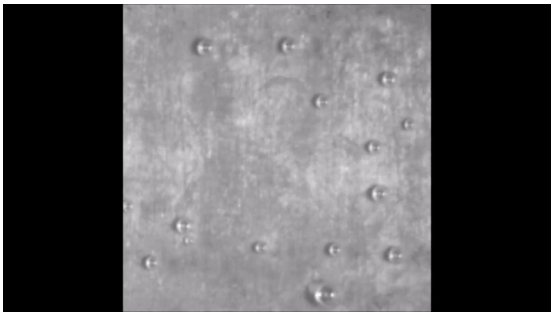

Video 1. High speed video from the top; bubble dynamics for horizontal flow boiling at 330 kg/m^2 s and 600 kW/m^2 and for smooth surface; playback 60 times slow motion; frame size 1.9x1.9 mm.

Laser etching used to manufacture the grooved surfaces in the present work induces two simultaneous changes to the boiling surface. First, it increases the heat exchange area; for both surfaces the increase in area is about the same, $A_{modified}/A_s = 1.08$. Second, it generates deformations and abnormalities at the edges of the grooves and creates also a micro-rough texture at the walls inside the grooves with roughness higher than that of the smooth surface. The above are in agreement with the findings of Sommers and Yerkes [10].

Fig. 4 displays top view images of bubbles for the two grooved surfaces at horizontal and vertical inclination and for similar working conditions (G, q″). These conditions are representative of the comparison between any combination of G and q"; moreover these specific conditions are chosen to be presented in Fig. 4 because they yield higher bubble density and larger bubbles sizes, and so illustrate better the discrepancies in the bubble dynamic behavior than other cases with fewer and smaller bubbles. When comparing the same surface at the two different inclinations, there aren't large macroscopic differences in bubbles number and sizes. On the contrary, when comparing surface #1 (grooves parallel to the flow) with surface #2 (grooves perpendicular to the flow) the former shows smaller bubbles inside the grooves and larger bubbles outside the grooves than the latter. In addition, inside the grooves a third type of bubbles appears compared to the two types mentioned above for the smooth (reference) surface, described in Supplementary 2. This refers to bubbles inside the grooves that grow to sizes much larger than bubbles outside the grooves. This is more so for surface #1. The shape of these large bubbles is elongated due to the restricted width of the grooves (420 μm). In addition, the effect of mass and heat flux on bubble dynamic behavior is only a matter of the number and size of bubbles and not of their type.

Enhanced bubble nucleation inside the grooves is attributed to two factors:

1. The edges of the grooves and the roughness/imperfections due to laser etching act as nucleation sites.
2. The exposed surface at the bottom of the grooves is 290 μm below the smooth boiling surface, which corresponds to about 0.2–0.9 °C higher local wall temperature (as calculated by Fourier law).

These two parameters, along with the small increase, ~8%, in the heat exchange area of the grooved surfaces result in much more intensified boiling compared to the smooth surface.

Representative behavior of bubbles interaction for the surfaces #1 and #2 is shown respectively in Supplementary 3 and 4 for the horizontal and in Supplementary 5 and 6 for the vertical channel inclination. They correspond to mass flux G = 330 kg/m^2 s and heat flux q″ = 800 kW/m^2. In all cases, more bubbles are present inside the grooves compared to the smooth surface because of the enhanced bubble nucleation described above, which attract their neighbors and coalescence and, eventually, detach and fully condense in the cold bulk liquid. No serious discrepancies are observed between horizontal and vertical inclination regarding the same surface.

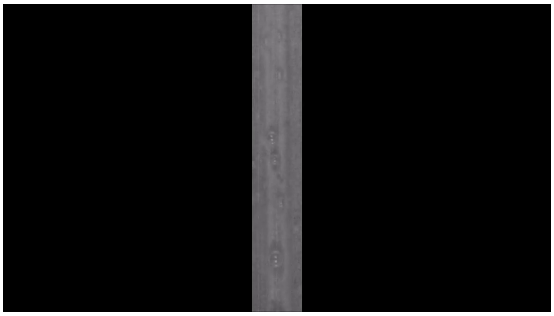

Video 2. High speed video from the top; bubble dynamics for horizontal flow boiling at 330 kg/m^2 s and 800 kW/m^2 and for surface #1; playback 60 times slow motion; frame size 0.8 × 4.9 mm.

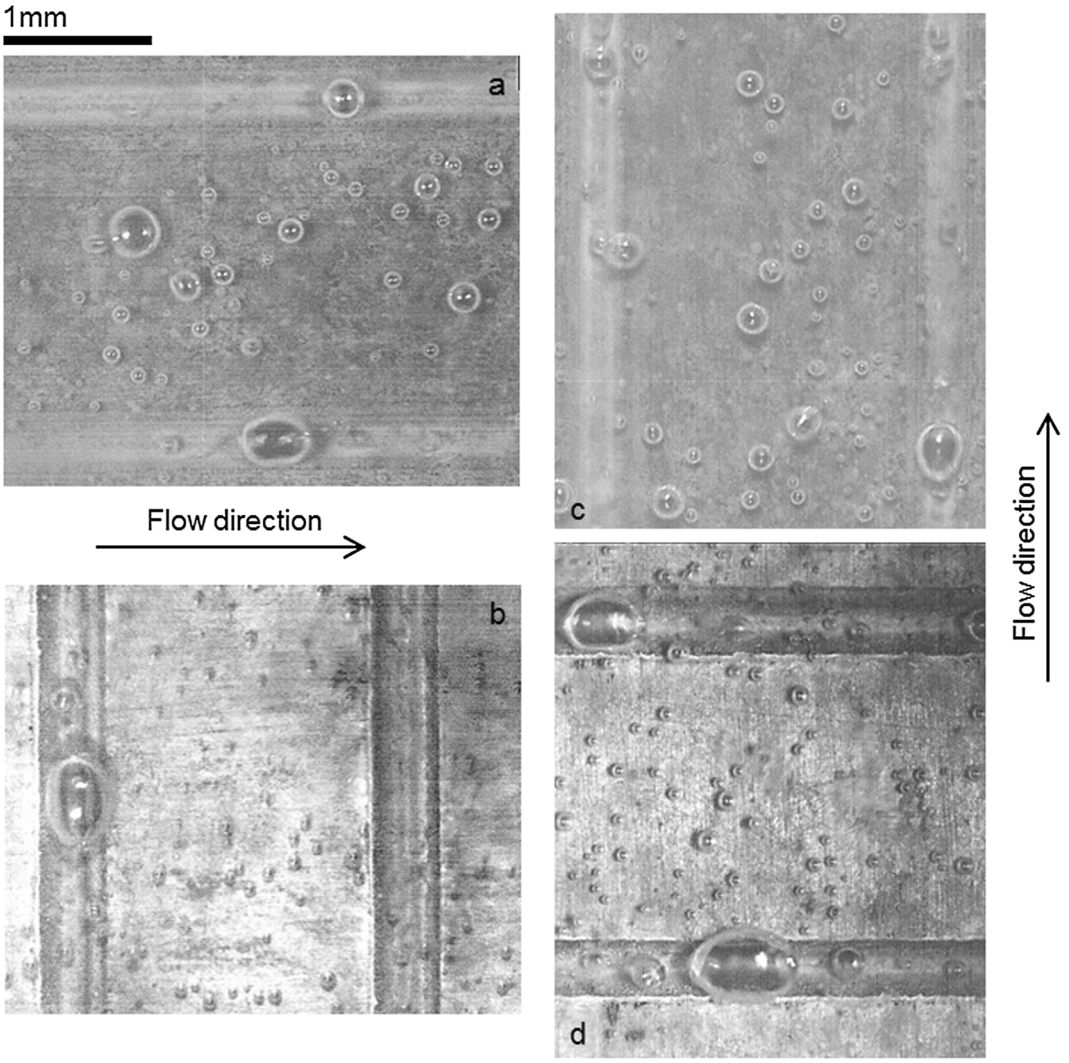

Fig. 4. Flow boiling visualizations from the top, for mass flux G = 330 kg/m^2 s, heat flux q″ = 800 kW/m^2 (a) surface #1, horizontal inclination, (b) surface #2, horizontal inclination, (c) surface #1, vertical inclination, and (d) surface #2, vertical inclination.

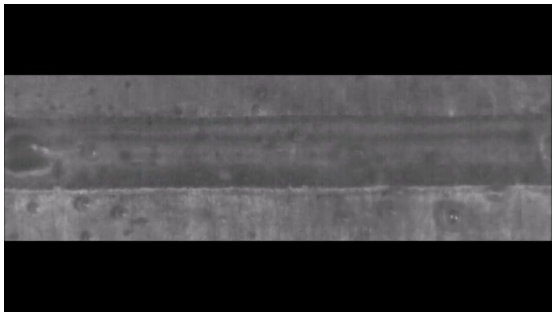

Video 3. High speed video from the top; bubble dynamics for horizontal flow boiling at 330 kg/m^2 s and 800 kW/m^2 and for surface #2; playback 60 times slow motion; frame size 3.3 × 1.0 mm.

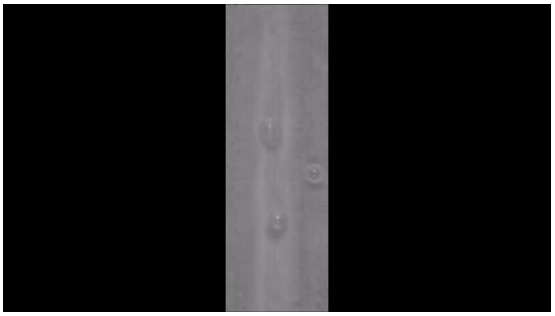

Video 4. High speed video from the top; bubble dynamics for vertical flow boiling at 330 kg/m^2 s and 800 kW/m^2 and for surface #1; playback 60 times slow motion; frame size 0.8 × 2.4 mm.

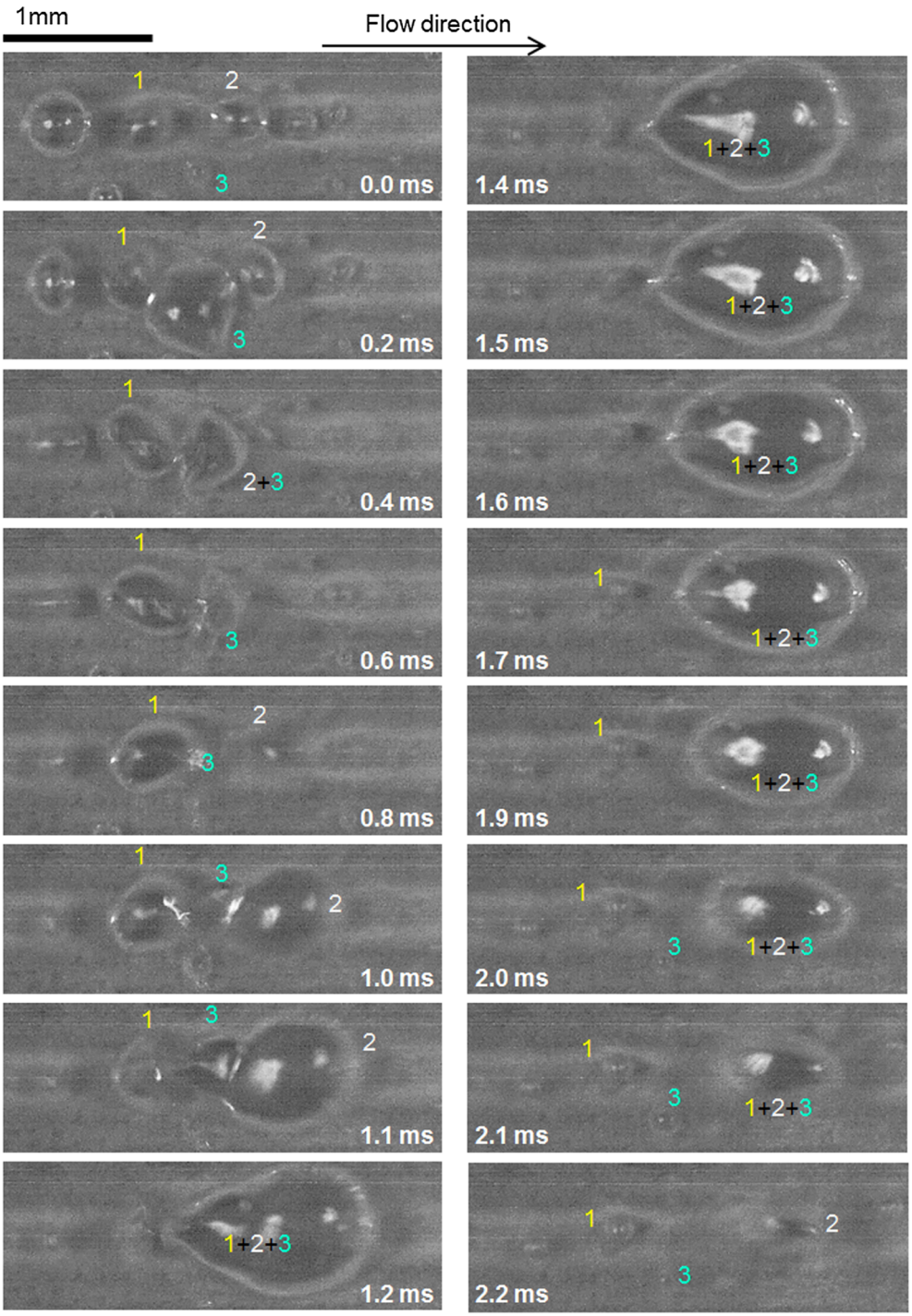

Fig. 5. Bubbles interaction inside a groove on surface #1, horizontal inclination, mass flux G = 330 kg/m^2 s and heat flux q″ = 800 kW/m^2. *Numbers next to bubbles help follow their changes through the frames' sequence.*

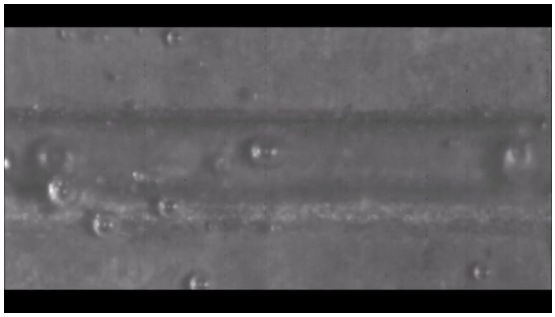

Video 5. High speed video from the top; bubble dynamics for vertical flow boiling at 330 kg/m^2 s and 800 kW/m^2 and for surface #2; playback 60 times slow motion; frame size 2.3 × 1.1 mm.

However, when comparing the two grooved surfaces to each other in Figs. 5 and 6, it is observed that bubbles interaction, involving coalescence, deformation and condensation, happens faster in surface #1. This feature might be explained by the fact that grooves parallel to the flow allow bubbles to slide along the grooves which causes bubbles to stand at every instant on a new surface spot which is apparently hotter than a fixed spot under pinned growing bubbles. Hotter surface means faster bubble growth. On the other hand, in surface #2, when bubbles that slide across the smooth area between neighboring grooves reach a groove, their foot detaches from the surface, regardless their size, and float in the liquid and then these bubbles condense partially or fully in the cold bulk liquid. The two modified surfaces yield different bubbles features, which result in different heat transfer performance, especially compared to the smooth reference surface. In the next sections evidence is provided on the extent of heat transfer enhancement that the modified surfaces bring.

3.2. Effect of surface morphology on boiling curves

The effect of surface morphology on boiling curves is examined for the horizontal and vertical channel inclination at three mass fluxes, G: 330, 630 and 830 kg/m^2 s (Fig. 7). In this Figure, the dashed lines represent a specific % shift to the left of the boiling curve for a smooth surface to quantify comparisons among curves. In most cases, the boiling curves for both grooved surfaces are shifted to lower wall superheats, compared to the smooth surface. Lines at q″ = 800 kW/m^2 are guides for the eye to allow comparisons between the corresponding ΔT_{wall} values for the different mass fluxes and inclinations.

In all graphs, the Onset of Nucleate Boiling (ONB) represents conditions of the first bubbles appearance on the boiling surface (determined by high speed imaging). In addition, the Onset of Bubbly Regime (OBR) represents the domination of nucleate boiling over forced convection and is identified by the abrupt rise in the slope of the boiling curve. ONB is depicted by a thick blue line. Likewise, OBR is depicted by a thick red line. These lines demarcate the areas of the dominant heat transfer mechanisms, which are:

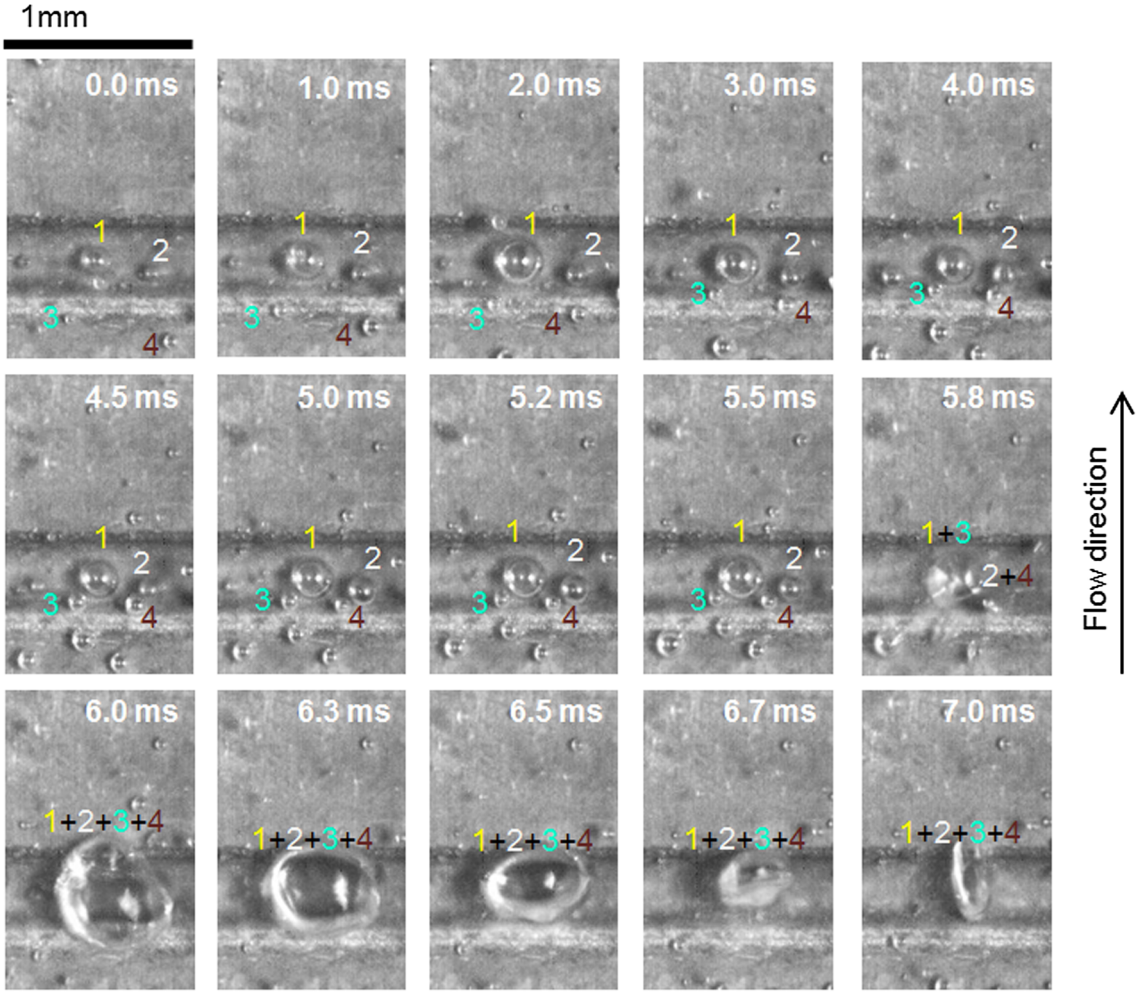

Fig. 6. Bubbles interaction inside a groove on surface #2, vertical inclination, mass flux G = 330 kg/m^2 s and heat flux q″ = 800 kW/m^2. *Numbers next to bubbles help follow their changes through the frames' sequence.*

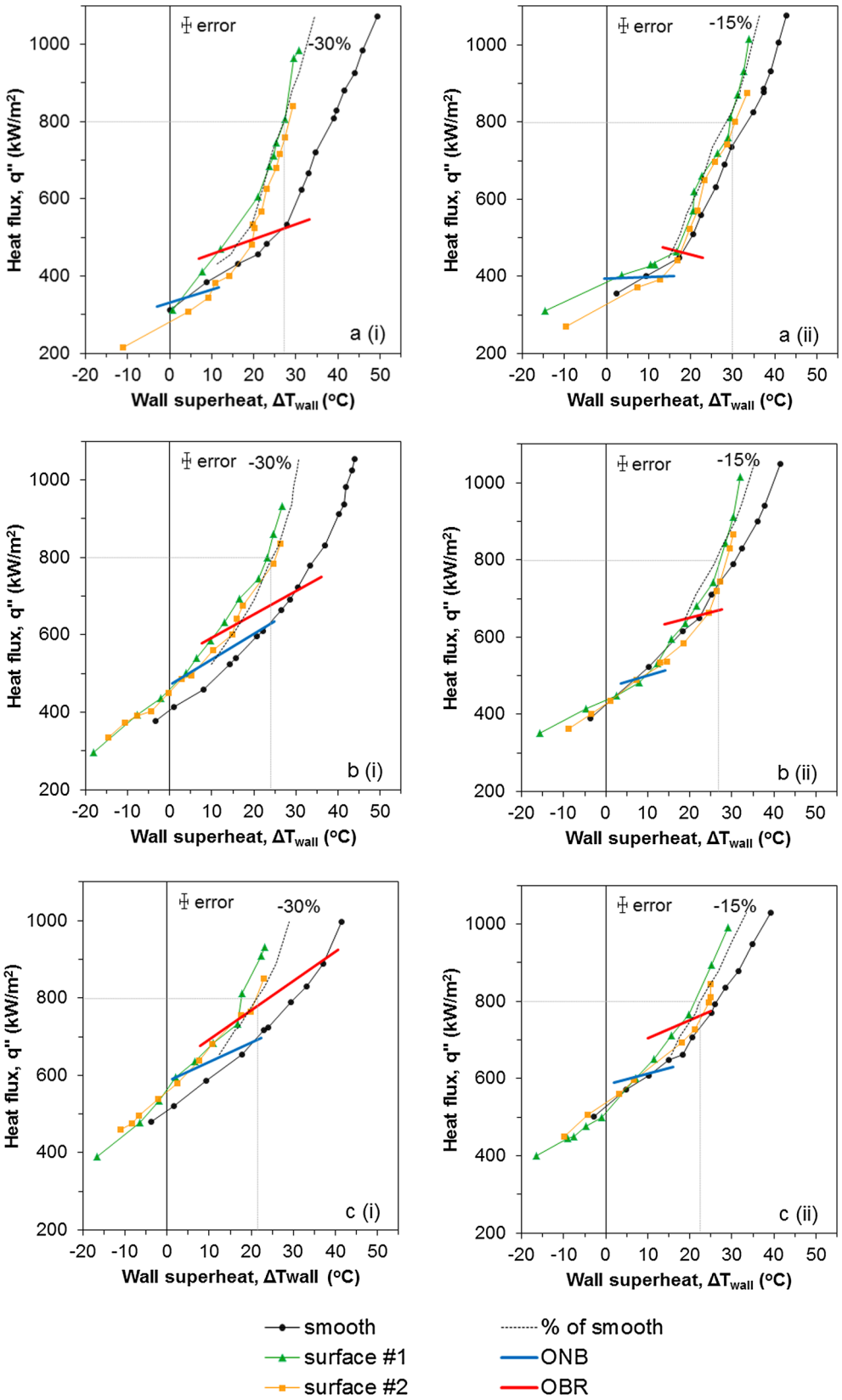

Fig. 7. Effect of surface morphology on boiling curves for (i) horizontal and (ii) vertical channel inclination and mass fluxes (a) 330, (b) 630 and (c) 830 kg/m^2 s. *ONB: onset of nucleate boiling, OBR: onset of bubbly regime. The dashed lines represent a specific % shift to the left of the boiling curve for a smooth surface.*

- Below ONB: there is single phase liquid flow where forced convective heat transfer dominates.
- Between ONB and OBR: boiling has started but forced convection still plays a significant role; so, heat transfer is attained by a combination of forced convection and nucleate boiling.
- Above OBR: there is intense boiling and bubbly flow dominates, so

Table 4
Wall superheat and heat flux for Onset of Nucleate Boiling (ONB) and Onset of Bubbly Regime (OBR).

G (kg/m^2 s)	Surface	ΔT_{wall} (°C) ONB	q″ (kW/m^2) ONB	ΔT_{wall} (°C) OBR	q″ (kW/m^2) OBR
Horizontal					
330	s	8.6	380	27.6	530
	#1	1.0	310	11.2	470
	#2	4.9	340	19.4	490
630	s	22.1	610	30.7	720
	#1	2.9	500	9.4	580
	#2	5.2	490	14.4	610
830	s	23.1	710	37.7	900
	#1	5.8	630	16.7	730
	#2	8.2	630	18.7	760
Vertical					
330	s	9.9	400	17.8	460
	#1	4.4	400	16.3	470
	#2	7.9	380	17.5	460
630	s	10.7	530	23.5	650
	#1	8.0	480	20.2	660
	#2	8.8	520	22.7	640
830	s	11.5	610	25.2	760
	#1	8.7	600	16.4	750
	#2	9.0	600	23.5	780

heat transfer is accomplished chiefly by nucleate boiling.

ONB and OBR lines in the graphs are only average indicators, while more precise data are displayed in Table 4. Increasing G decreases thermal boundary layer thickness, enhances forced convective mechanism and delays ONB and OBR [13,19]. Compared to the smooth surface, the points at which ONB and OBR occur for the grooved surfaces are at lower q" and/or ΔT_{wall} due to the peculiarities of the grooves as mentioned above (edges, rough walls, increased bottom temperature). For surface #1, it is worth mentioning that boiling initiates even at a ΔT_{wall} as low as 1 °C (wall average value), 330 kg/m^2 s and horizontal inclination, Fig. 7a(i), despite the high degree of subcooling (ΔT_{sub} = 70 °C) which would be expected to "delay" boiling [20,21]. As seen in Table 4, this corresponds to an 88% decrease in ΔT_{wall} for ONB with respect to the value for the smooth surface; this decrease is also high for the other two mass fluxes (87% for 630 kg/m^2 s and 75% for 830 kg/m^2 s). Vertical inclination of surface #1 yields decreases in ΔT_{wall} for ONB between 25 and 60% for all the examined mass fluxes, Table 4. A similar effect (40% decrease in ΔT_{wall} for ONB) was also observed by Hsieh and Lin [22], with 75 °C subcooled water at 820 kg/m^2 s and a 2 μm diamond film covering their copper surface. Surface #2 results in smaller decreases of ONB for both horizontal (45–75%) and vertical inclination (18–20%) (Table 4). If percentages are averaged to represent both grooved surfaces, these would be ~70% decrease of ΔT_{wall} (ONB) for the horizontal and ~30% decrease for the vertical inclination.

Summarizing, in terms of the ΔT_{wall} for ONB (but also OBR), both grooved surfaces lead to smaller values than the smooth surface, this being more evident at the horizontal inclination. This is attributed to the intense bubbles dynamics induced by the grooves. Nevertheless, surface #1 leads to only marginally smaller ΔT_{wall} for ONB (and OBR) than surface #2 at both inclinations. Therefore, the different features of bubbles behavior at the two grooved surfaces seem to enhance comparably heat transfer performance with regards the smooth surface.

3.3. Effect of surface morphology on average heat transfer coefficient

Fig. 8 shows the effect of surface morphology on the variation of heat transfer coefficient, h, versus heat flux, q". Regions where the slope of the curves rises imply conditions where nucleate boiling mechanism dominates and so h is very much q" dependent. Interestingly, in some cases, e.g. 330 and 630 kg/m^2 s at the horizontal inclination (Fig. 8a(i) and b(i)), the slopes of the curves are large even below the designated ONB. This means that boiling has actually initiated at lower q" than the one implied by ONB. Although such behavior is rather not expected due to the high ΔT_{sub} and the low ΔT_{wall}, the possibility cannot be excluded that micro-bubbles may have appeared before ONB but they were too small to be visually detected while they were capable of giving a measurable effect on heat transfer. Previous works have shown that indeed surface treatment can cause extensive bubble nucleation of this scale [23] and also hasten ONB [24].

In Fig. 8, water outlet temperature with respect to q" is illustrated at inset plots. In most cases, the water outlet temperature does not vary significantly between the smooth and the grooved surfaces. Yet, for the horizontal inclination the two grooved surfaces yield clearly higher water temperature at the outlet than for the vertical inclination. This is something quite expected due to the larger shift in the boiling curves for the horizontal inclination (Fig. 7; higher q″ at the same ΔT_{wall}, more intense boiling).

Fig. 9 shows that enhancement of h for the grooved surfaces compared to the smooth one. For the horizontal inclination the enhancement never exceeds ~17% for all the examined mass fluxes. The corresponding maximum enhancement of h for the vertical inclination is less than ~7%. Taking into account the error bar in the estimation of h, surface modification has a small impact on h for the vertical inclination, actually this being evident only at the higher q″, i.e. above the OBR. On the average, the examined grooved surfaces enhance flow boiling heat transfer coefficient by ~10% for the horizontal and by ~2.5% for the vertical upward flow, compared to a smooth surface The nearly 10% difference in the performance of grooved surfaces between horizontal and vertical channel inclination is similar to the almost 10% difference in the performance of the smooth surface between this two inclinations [19]. So, one might argue that the effect of inclination is strong and independent of surface modification.

4. Conclusion

The heat transfer performance of highly subcooled water flow boiling on two micro-grooved copper surfaces is investigated. Surfaces are produced by laser engraving. Surface #1 has grooves parallel to the flow whereas surface #2 perpendicular to the flow. Both grooved surfaces yield better heat transfer performance than a reference smooth

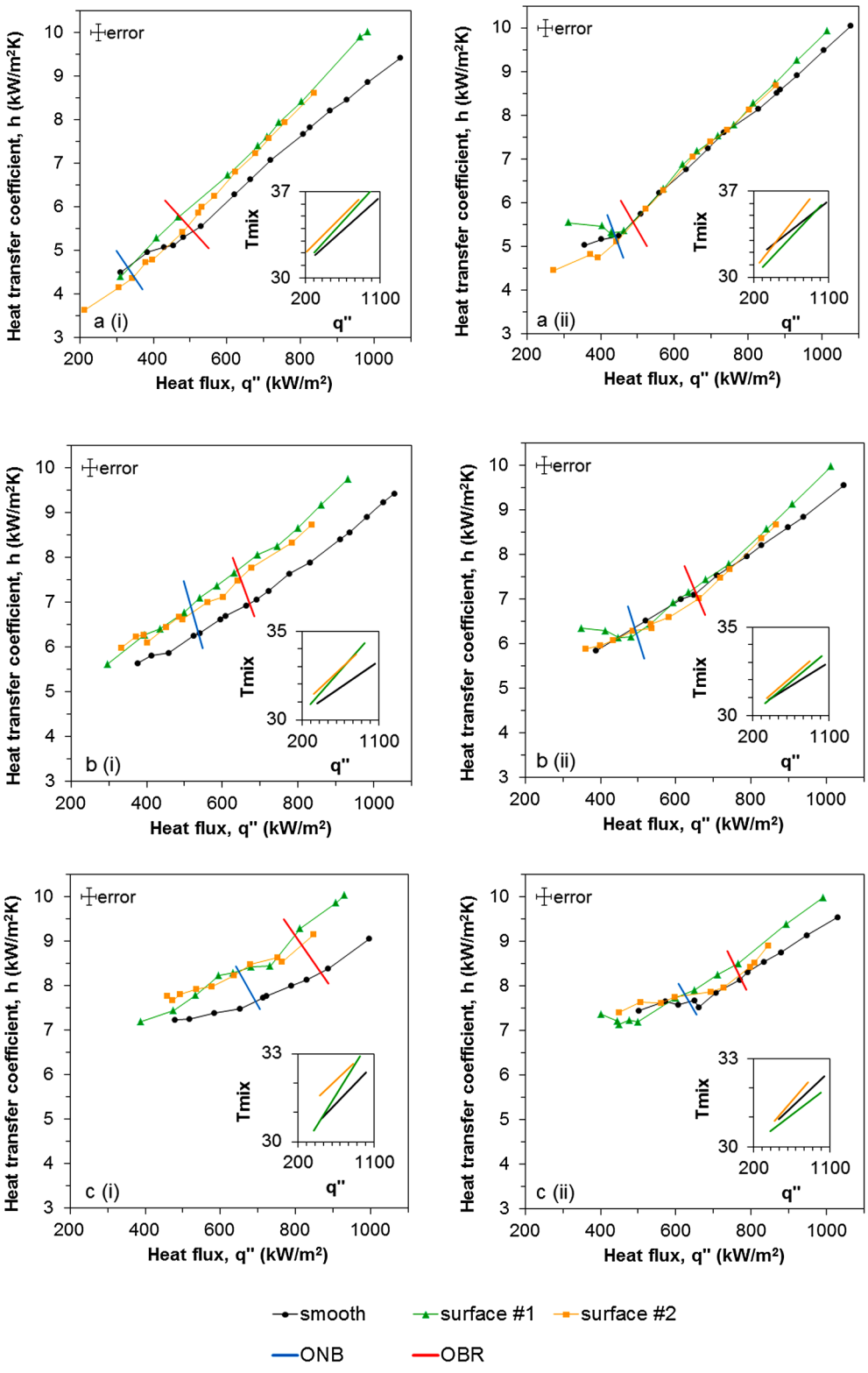

Fig. 8. Effect of surface morphology on heat transfer coefficient for (i) horizontal and (ii) vertical channel inclination and mass fluxes (a) 330, (b) 630 and (c) 830 kg/m^2 s. *Inset plots: Effect of surface morphology on water outlet temperature (T_{mix}).*

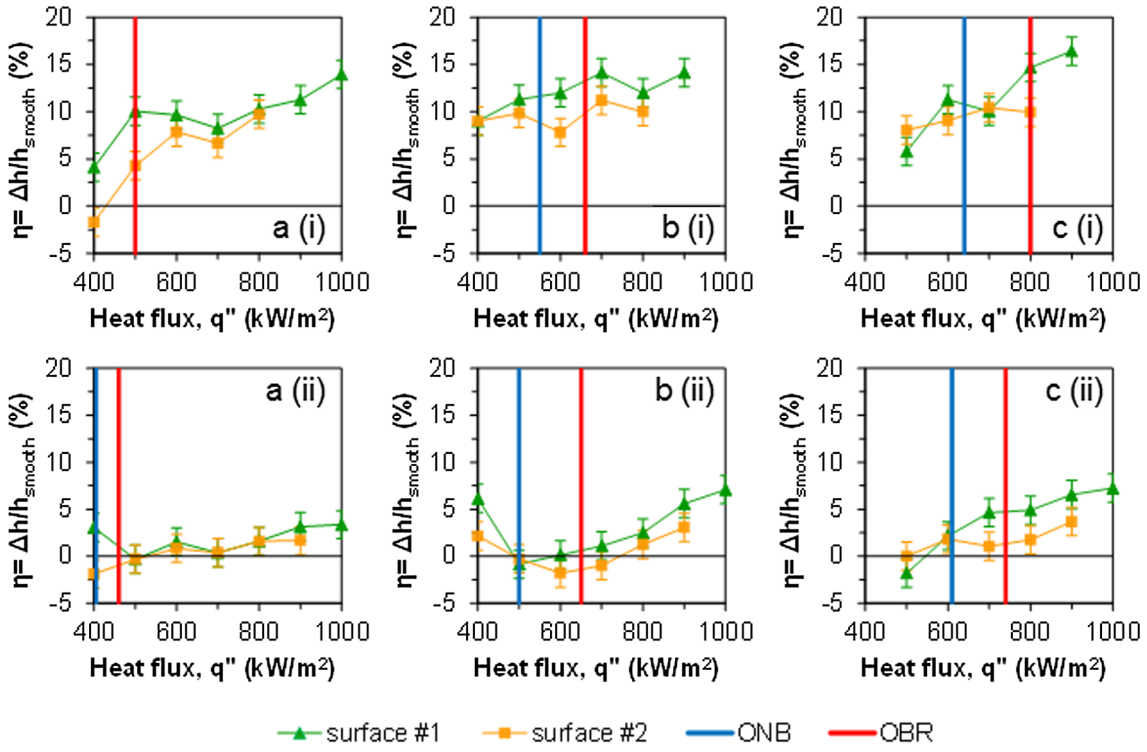

Fig. 9. Effect of surface morphology on the percentage change of heat transfer coefficient for (i) horizontal and (ii) vertical channel inclination and mass fluxes (a) 330, (b) 630 and (c) 830 kg/m^2 s. *ONB: onset of nucleate boiling, OBR: onset of bubbly regime.*

surface which is clearly above the ~8% higher heat exchange area offered by the grooves. On the other hand, the two grooved surfaces show similar heat transfer performance to each other despite the different bubbles behavior observed in each grooved surface. Yet, for each grooved surface the performance differs between horizontal and vertical inclination:

- The grooved surfaces lead to early boiling initiation, despite the high subcooling (ΔT_{sub} = 70 °C); ΔT_{wall} (ONB) drops ~70% for the horizontal and ~30% for the vertical inclination (average values of the two micro-grooved surfaces for all mass fluxes).
- The boiling curves of the grooved surfaces for the horizontal inclination are shifted to 30% lower ΔT_{wall} than the smooth surface, and for the vertical inclination to 15% lower ΔT_{wall}.
- The heat transfer coefficient of the grooved surfaces for the horizontal inclination is 10–15% higher and for the vertical inclination 5–7% higher than the smooth surface (with an error of 3%).
- Heat transfer enhancement of the grooved surfaces is attributed to the enhanced bubble nucleation inside the grooves due to the imperfections of laser treatment and to the locally higher temperature inside the grooves (290 μm below the baseline level of the smooth surface).
- Deviations of the heat transfer performance of the grooved surfaces between horizontal and vertical inclination are ~10% which are similar to respective deviations of the smooth surface. Thus the effect of inclination is strong and independent of surface modification.

Acknowledgements

This research was supported by the European Space Agency (Contract No. 4000106405/12/NL/PA on highly efficient flow boiling macrostructured/ macroporous channels), and EPAnEK 2014-2020 Operational Programme, Competitiveness, Entrepreneurship, Innovation.

References

[1] S.M. Ghiaasiaan, Two-phase flow, boiling and condensation in conventional and miniature systems, Cambridge University Press, New York, 2008.
[2] A.E. Bergles, Techniques to enhance heat transfer, in: W. Rohsenow, J.P. Hartnett, Y.I. Cho (Eds.), Handbook of Heat Transfer, McGraw-Hill, New York, 1998, pp. 11.11–11.76.
[3] Z. Wu, B. Sundén, On further enhancement of single-phase and flow boiling heat transfer in micro/minichannels, Renew. Sust. Energy Rev. 40 (2014) 11–27.
[4] M.C. Vlachou, J.S. Lioumbas, T.D. Karapantsios, Heat transfer enhancement in boiling over modified surfaces: A critical review, Interfacial Phenom Heat Transf. 3 (4) (2015) 341–367.
[5] S. Mori, Y. Utaka, Critical heat flux enhancement by surface modification in a saturated pool boiling: A review, Int. J. Heat Mass Transfer. 108 (2017) 2534–2557.
[6] W.-L. Cheng, H. Chen, S. Yuan, Q. Zhong, Y.-F. Fan, Experimental study on heat transfer characteristics of R134a flow boiling in "Ω"-shaped grooved tube with different flow directions, Int. J. Heat Mass Transf. 108 (2017) 988–997.
[7] L. Wang, A.R. Khan, N. Erkan, H. Gong, K. Okamoto, Critical heat flux enhancement on a downward face using porous honeycomb plate in saturated flow boiling, Int. J. Heat Mass Transf. 109 (2017) 454–461.
[8] C. Haas, F. Kaiser, T. Schulenberg, T. Wetzel, Critical heat flux for flow boiling of water on micro-structured Zircaloy tube surfaces, Int. J. Heat Mass Transf. 120 (2018) 793–806.
[9] P.A. Raghupathi, S.G. Kandlikar, Pool boiling enhancement through contact line augmentation, Appl. Phys. Lett. 110 (20) (2017) 204101.
[10] A.D. Sommers, K.L. Yerkes, Using micro-structural surface features to enhance the convective flow boiling heat transfer of R-134a on aluminum, Int. J. Heat Mass Transf. 64 (2013) 1053–1063.
[11] M. Rahman, J. Pollack, M. Mc, Carthy, Increasing boiling heat transfer using low conductivity materials, Sci. Rep. 5 (2015) 13145.
[12] M.M. Rahman, M. McCarthy, Effect of length scales on the boiling enhancement of structured copper surfaces, J. Heat Transf. 139 (11) (2017) 111508.
[13] M.C. Vlachou, J.S. Lioumbas, K. David, D. Chasapis, T.D. Karapantsios, Effect of channel height and mass flux on highly subcooled horizontal flow boiling, Exp. Therm. Fluid Sci. 83 (2017) 157–168.
[14] M.C. Paz, M. Conde, E. Suárez, M. Concheiro, On the effect of surface roughness and material on the subcooled flow boiling of water: Experimental study and global correlation, Exp. Therm. Fluid Sci. 64 (2015) 114–124.
[15] V. Gnielinski, New equations for heat and mass transfer in turbulent pipe and channel flow, Int. Chem. Eng. 16 (2) (1976) 359–368.
[16] B.N. Taylor, C.E. Kuyatt, Guidelines for Evaluating and Expressing the Uncertainty of NIST Measurement Results, in: Technical Note 1297, National Institute of Standards and Technology, Gaithersburg, 1994.
[17] Z. Liu, E.H.S. Winterton, A general correlation for saturated and subcooled flow boiling in tubes and annuli, based on a nucleate pool boiling equation, Int. J. Heat Mass Transf. 32 (11) (1991) 2759–2766.

[18] M.M. Shah, New correlation for heat transfer during subcooled boiling in plain channels and annuli, Int. J. Therm. Sci. 112 (2017) 358–370.
[19] M.C. Vlachou, T.D. Karapantsios, Effect of channel inclination on heat transfer and bubble dynamics during subcooled flow boiling, Int. J. Therm. Sci. 124 (2018) 484–495.
[20] K. Suzuki, H. Saitoh, K. Matsumoto, High heat flux cooling by microbubble meission boiling, Ann. NY Acad. 974 (2002) 364–377.
[21] C.R. Kharangate, L.E. O'Neill, I. Mudawar, M.M. Hasan, H.K. Nahra, R. Balasubramaniam, N.R. Hall, A.M. Macner, J.R. Mackey, Effects of subcooling and two-phase inlet on flow boiling heat transfer and critical heat flux in a horizontal channel with one-sided and double-sided heating, Int. J. Heat Mass Transf. 91 (2015) 1187–1205.
[22] S.-S. Hsieh, C.-Y. Lin, Subcooled convective boiling in structured surface micro-channels, J. Micromech. Microeng. 20 (1) (2010) 015027.
[23] H. Jo, S. Kim, H. Kim, J. Kim, M. Kim, Nucleate boiling performance on nano/microstructure with different wetting surfaces, Nanoscale Res. Lett. 7 (1) (2012) 242.
[24] J.M. Kim, S.H. Kang, D.I. Yu, H.S. Park, K. Moriyama, M.H. Kim, Smart surface in flow boiling: Spontaneous change of wettability, Int. J. Heat Mass Transf. 105 (2017) 147–156.